

pH-Switchable phenylalanine-templated copper nanoclusters: CO₂ probing and efficient peroxidase mimicking activity

Shashi Shekhar, Raibat Sarker,[‡] Paritosh Mahato,[‡] Sameeksha Agrawal and Saptarshi Mukherjee*

Department of Chemistry, Institute of Science Education and Research Bhopal, Bhopal Bypass Road, Bhopal 462 066, Madhya Pradesh, India.

**Corresponding author. E-mail: saptarshi@iiserb.ac.in; orcid.org/0000-0001-8280-0754*

‡Authors contributed equally.

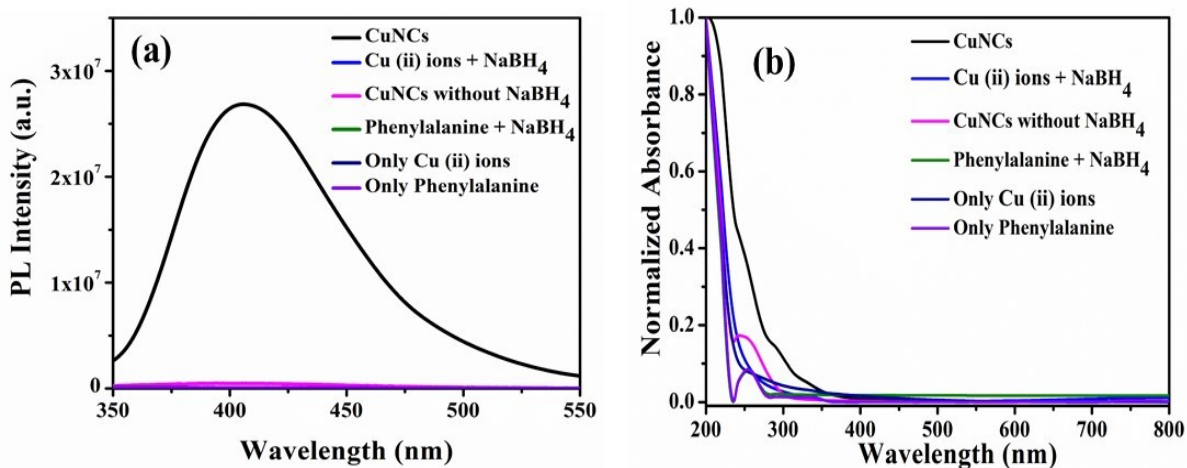


Fig. S1 Control experiments for characterizing the formation of Phe-templated B-CuNCs. (a) Emission spectra at 290 nm excitation of the Phe-templated CuNCs solution and various controls, as mentioned in the figure. (b) Absorbance spectra for CuNCs solution and various controls, as mentioned in the figure.

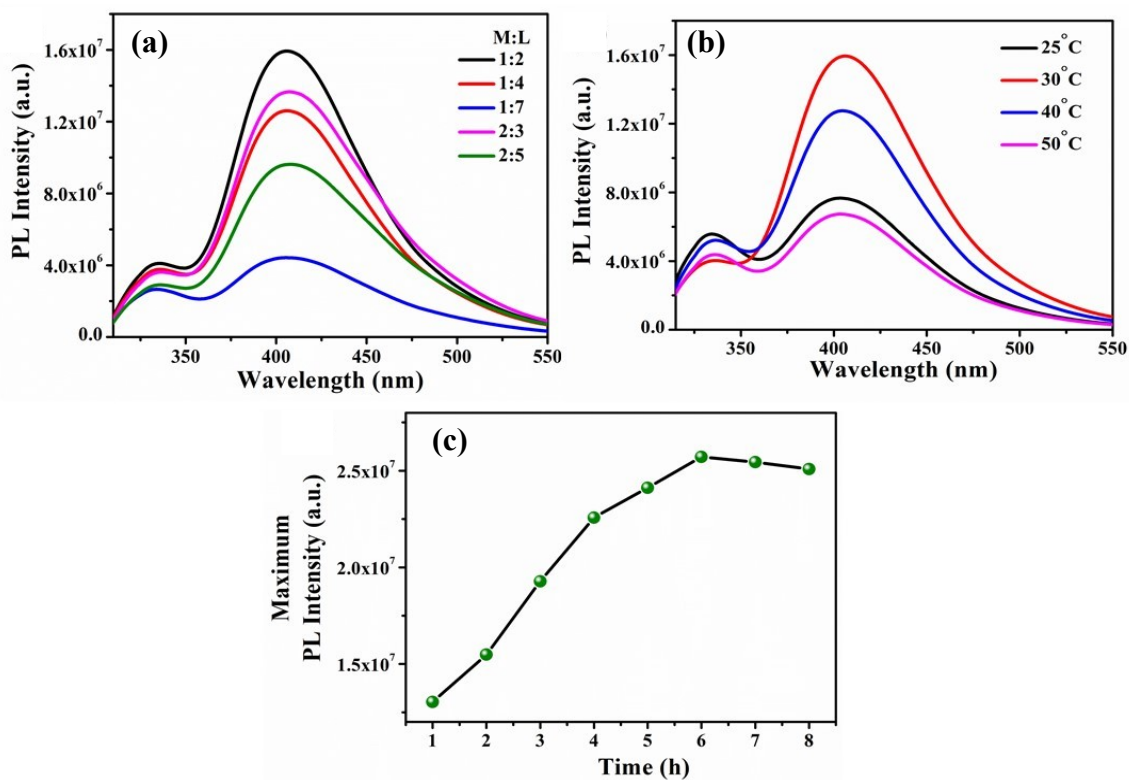


Fig. S2 Optimization of reaction conditions (a) PL spectra of B-CuNCs at 290 nm excitation wavelength for different M:L concentration ratios. (b) Variation in the PL spectra as a function of temperature as marked in the figure. (c) Variation in the maximum PL intensity spectra as a function of time as marked in the figure.

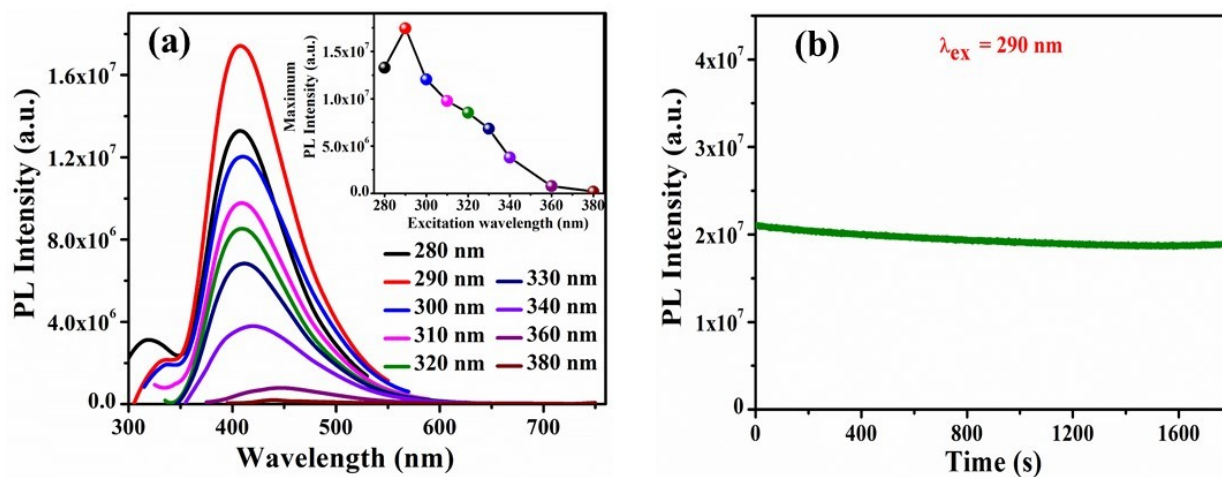


Fig. S3 (a) The excitation-dependent emission spectrum of the B-CuNCs; inset represents the variation of maximum PL intensity with excitation wavelengths. (b) The variation of PL intensity against time of the B-CuNCs substantiate the high photostable nature of the NCs; the emission was monitored at 410 nm when excited at 290 nm.

Table S1 Lifetime decay parameters for Phe-templated CuNCs at pH~4.

τ_1 (ns)	α_1	$\langle\tau\rangle^a$ (ns)	χ^2
2.61	1.00	2.61	1.09

^a±5%

Table S2 Assigned intense peaks in ESI mass spectra of CuNCs and their most probable compositions. Here, Phe = Phenylalanine (mol. wt. = 165.19 g mol⁻¹).

Assigned peaks (from Fig. 1c)	m/z	Composition
(1)	1210.22	[Cu ₈ (Phe) ₄ + 2Na - 2H] ⁻
(2)	1601.28	[Cu ₇ (Phe) ₇] ⁻

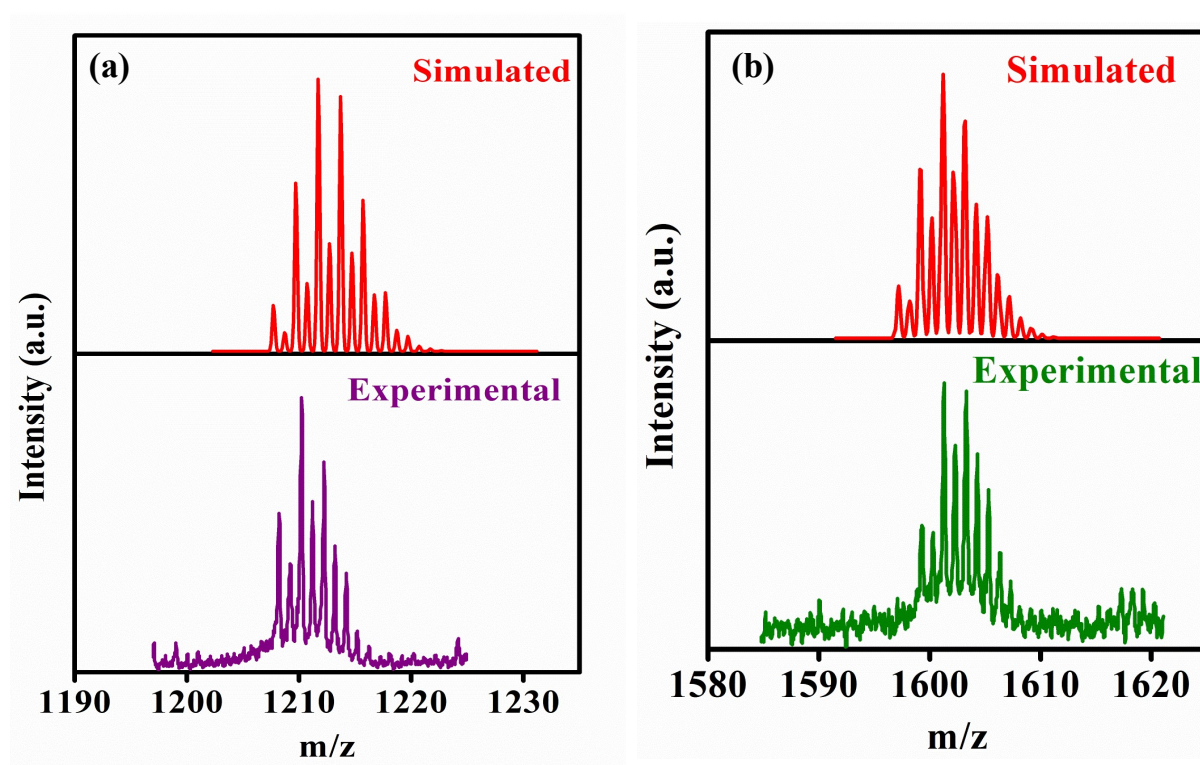


Fig. S4 Experimental and simulated isotopic distribution patterns of CuNCs corresponding to the peaks at m/z (a) 1210.22 (please refer to peak (1) of Fig. 1c and Table S2) and (b) 1601.28 (please refer to peak (2) of Fig. 1c and Table S2), respectively.

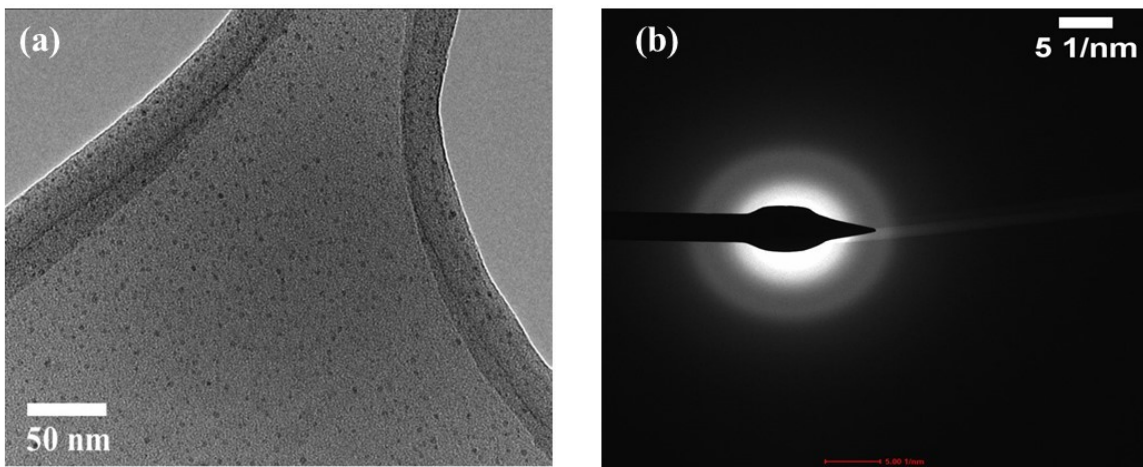


Fig. S5 (a) TEM image of CuNCs at 50 nm scale bar. (b) Selected Area Electron Diffraction (SAED) image of CuNCs.

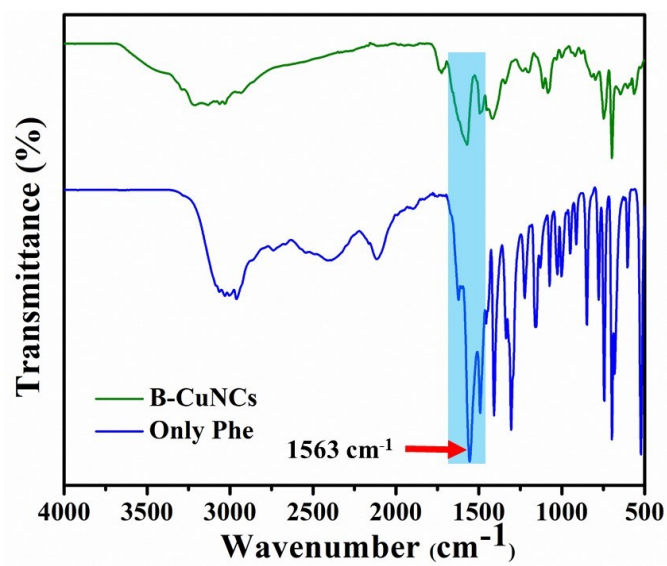


Fig. S6 FTIR spectra for Phenylalanine and B-CuNCs. At pH \sim 4, the role of the carboxylic group is seen involved during the formation of the CuNCs (as the stretching frequency \sim 1563 cm^{-1} is attenuated).

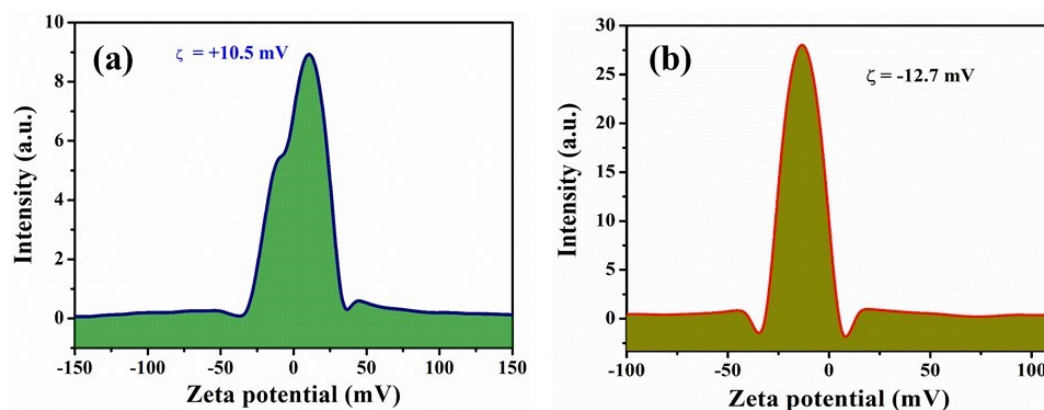


Fig. S7 Surface charge determination *via* zeta potential measurement for Phe-templated CuNCs. (a) B-CuNCs at pH \sim 4. (b) C-CuNCs at pH \sim 12.

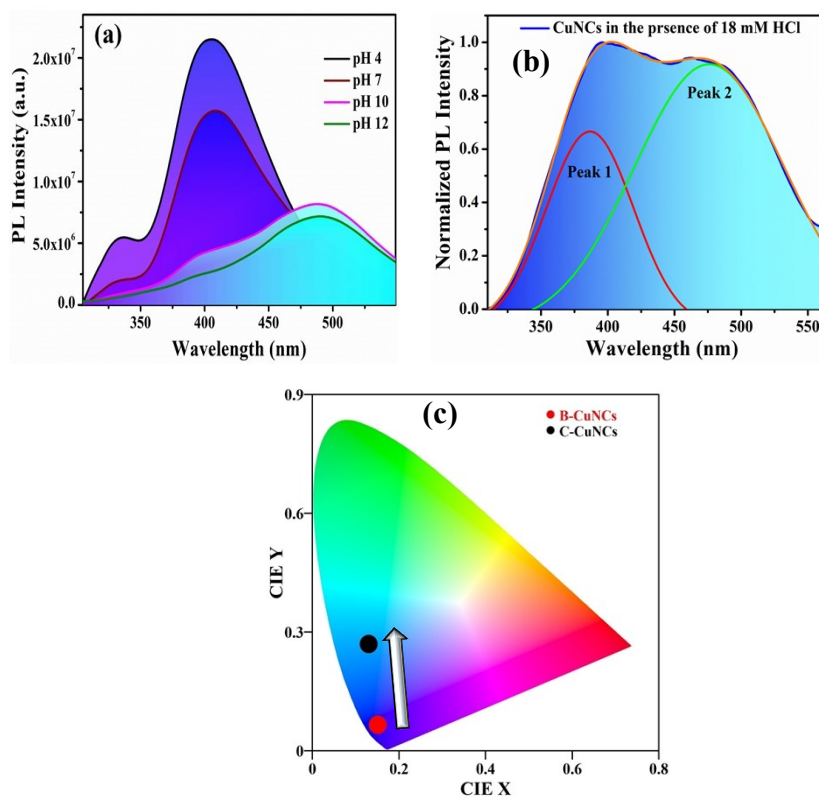


Fig. S8 (a) pH-dependent spectra of CuNCs. (b) Partial peak fitting of CuNCs in the presence of 18 mM HCl. The data signify the transition state involved during the intercluster conversion. (c) CIE coordinate plot for blue and cyan emitting CuNCs at pH~4 (0.15, 0.06) and pH~12 (0.13, 0.27).

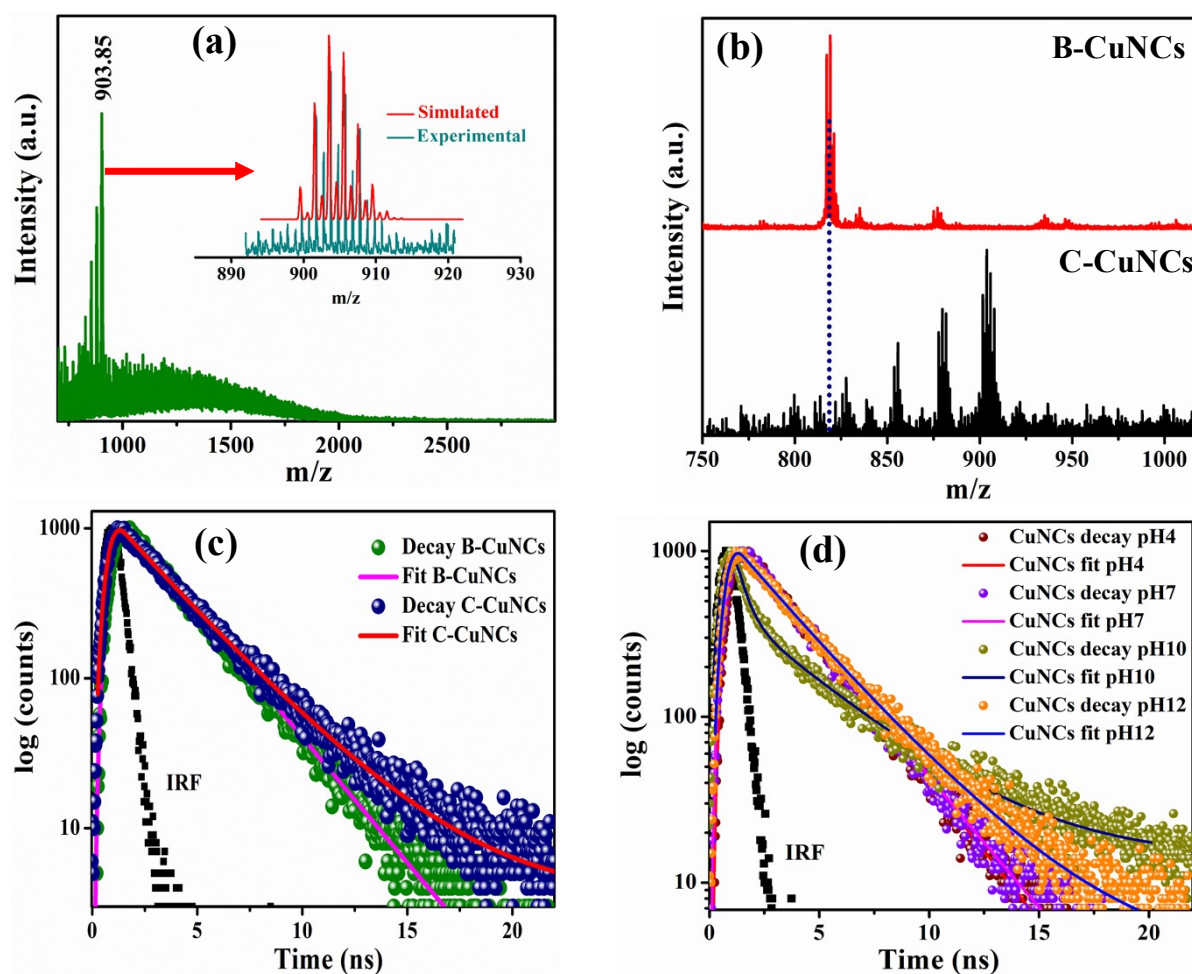


Fig. S9 (a) ESI mass spectrum of cyan emitting C-CuNCs at pH ~12. Inset represents the experimental and simulated isotopic distribution pattern corresponding to $m/z \sim 903.85$. (b) Comparison of ESI mass spectra of blue (B-CuNCs) and cyan emitting (C-CuNCs). (c) Lifetime decay profiles of blue (B-CuNCs) and cyan emitting (C-CuNCs) at pH 4 and 12, respectively. (d) pH-dependent lifetime decay profiles of CuNCs.

Table S3 Lifetime decay parameters for Phe-templated CuNCs at different pH.

pH	τ_1 (ns)	τ_2 (ns)	α_1	α_2	$\langle\tau\rangle^a$ (ns)	χ^2
7	2.69	-	1	-	2.69	1.06
10	0.48	3.99	0.28	0.72	3.01	1.06
12	2.47	3.79	0.56	0.44	3.05	1.07

^a $\pm 5\%$

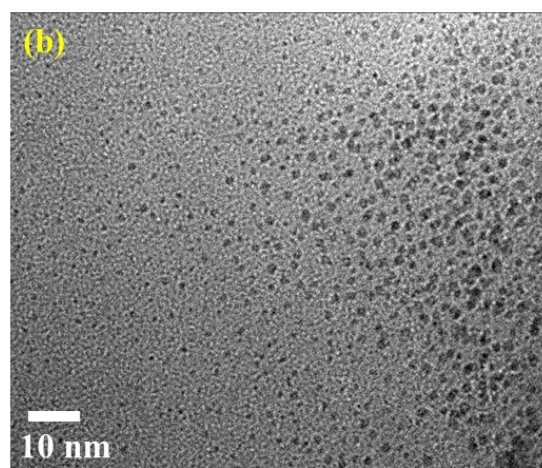
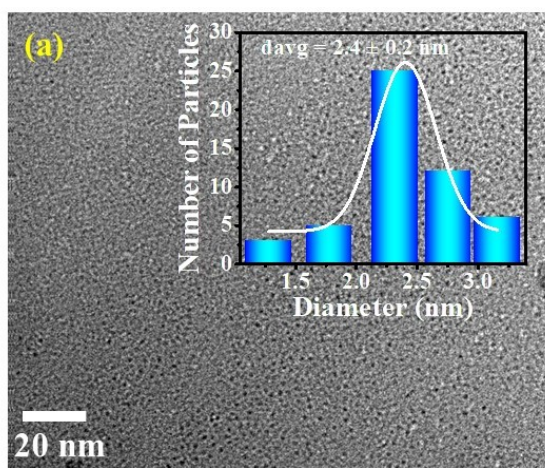


Fig. S10 TEM images of C-CuCNs, pH ~12. (a) at 20 nm and (b) 10 nm scale bars. The inset in (a) represents the particle size distribution of the C-CuNCs, depicting an average diameter of 2.4 ± 0.2 nm.

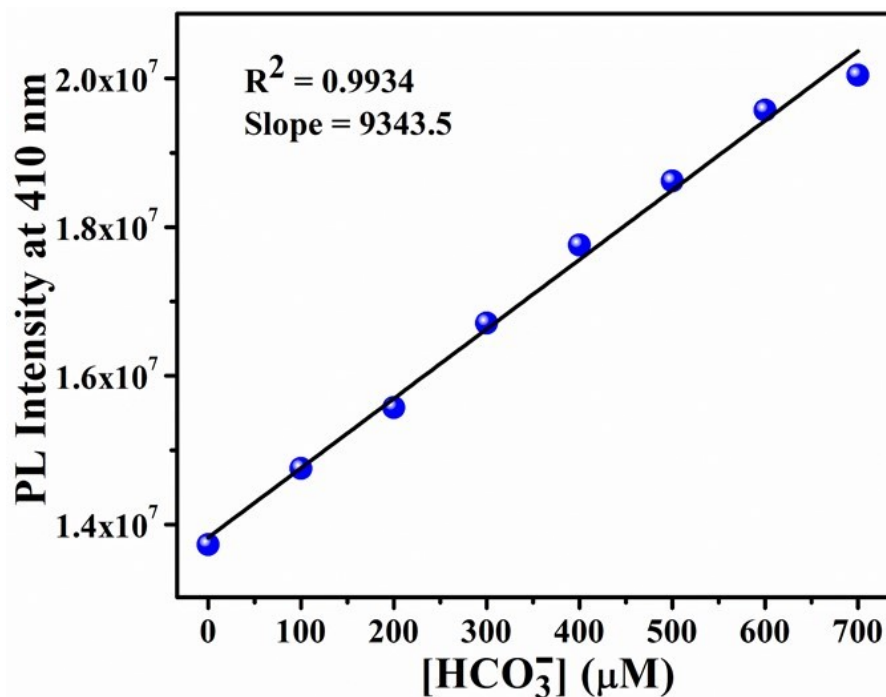


Fig. S11 Calibration curve for the estimation of LOD value using B-CuNCs in the presence of bicarbonate ions.

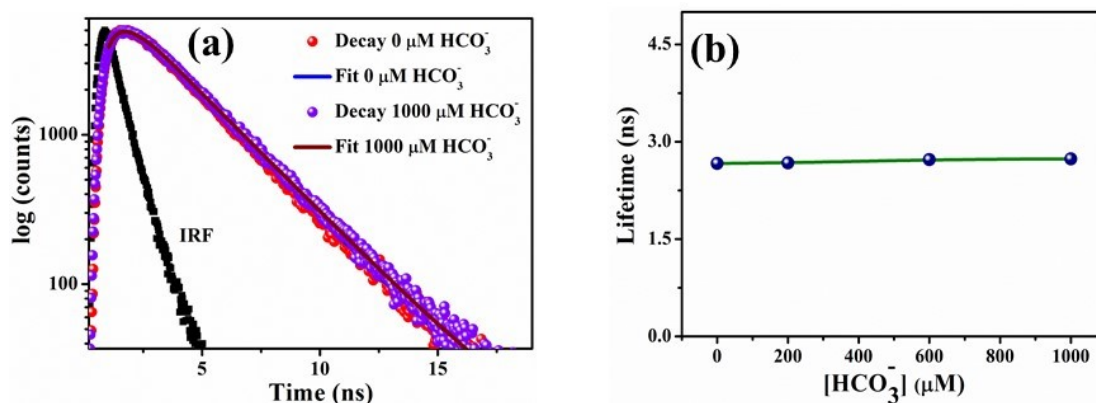


Fig. S12 (a) Lifetime decay profiles of B-CuNCs in the absence and presence of 1000 µM HCO₃⁻ ions. (b) Plot representing the non-variant nature of lifetime values of B-CuNCs as a function of [HCO₃⁻] ions.

Table S4 Lifetime parameters of Phe-templated B-CuNCs with different concentration of HCO_3^- ions

$[\text{HCO}_3^-]$	τ_1 (ns)	α_1	χ^2	$\langle\tau\rangle^a$ (ns)
0	2.66	1.00	1.07	2.66
200	2.67	1.00	1.09	2.67
600	2.72	1.00	1.05	2.72
1000	2.73	1.00	1.07	2.73

^a $\pm 5\%$

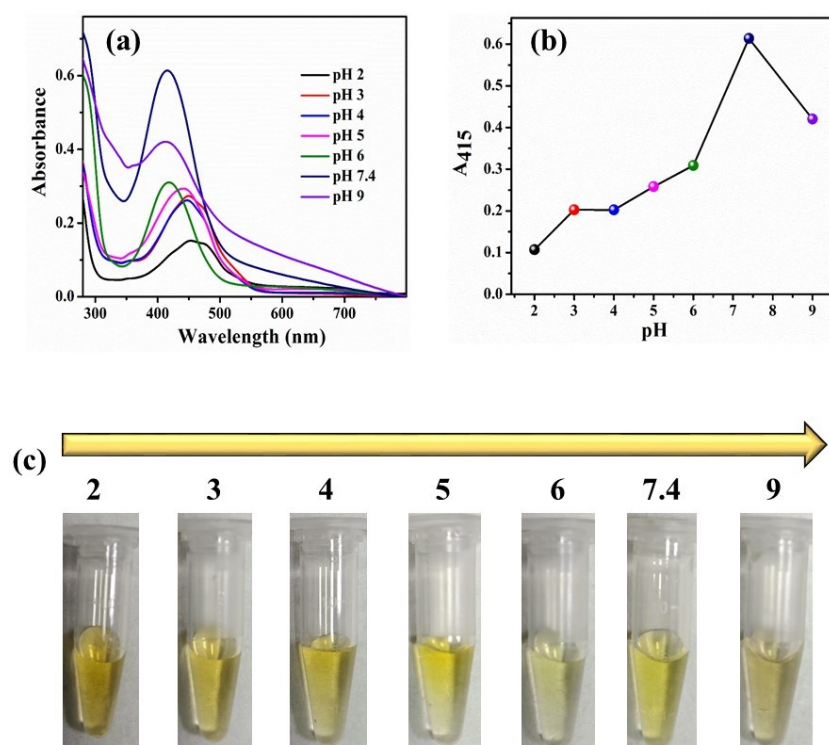


Fig. S13 (a) Optimization of pH for the peroxidase-like activity of B-CuNCs. (b) Change in absorbance values monitored at 415 nm as a function of pH. (c) Photographic images display visual color change that takes place after the catalytic reaction with the variation of the pH of the solution.

([OPD] = 0.2 mM, [H₂O₂] = 10 mM, and [B-CuNCs] = 17 μM were maintained during the experiments).

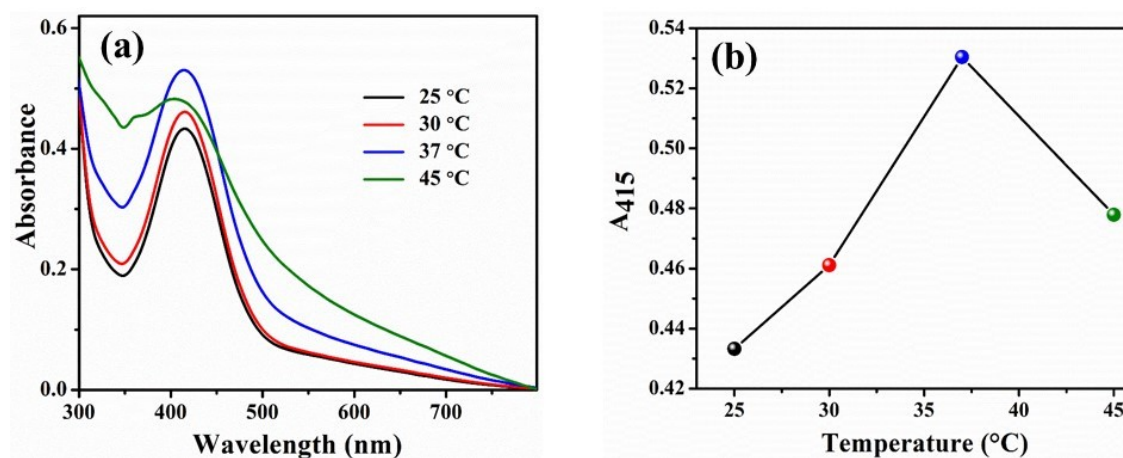


Fig. S14 (a) Optimization of the temperature for the peroxidase-like activity of B-CuNCs. (b) Change in absorbance values monitored at 415 nm as a function of temperature. ([OPD] = 0.2 mM, [H₂O₂] = 10 mM, [B-CuNCs] = 17 μM, and pH = 7.4 were maintained during the experiments).

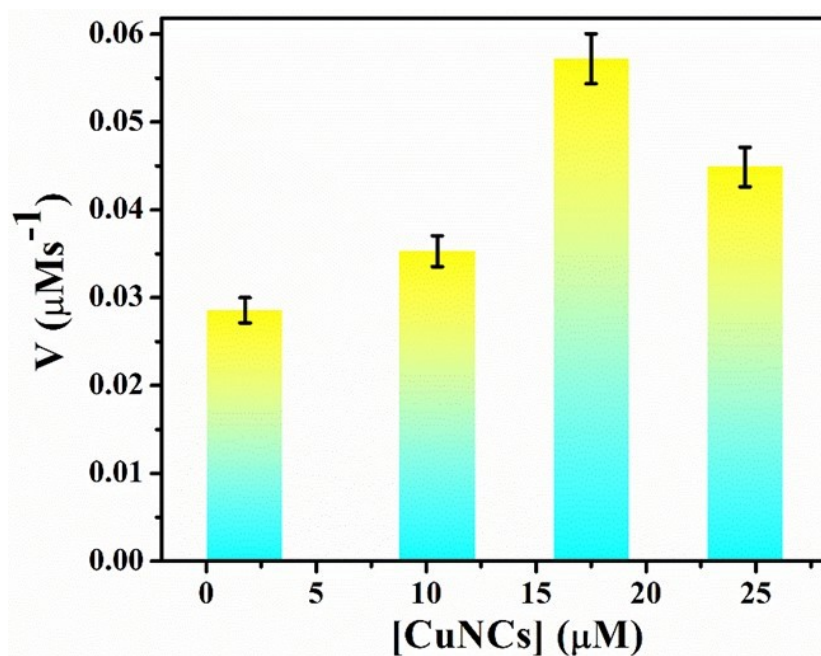
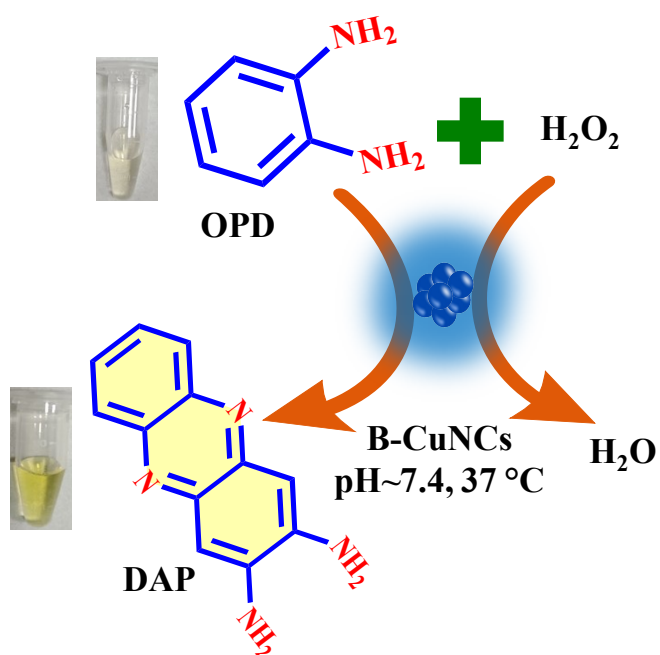


Fig. S15 Optimization of the concentration of B-CuNCs to achieve the maximum catalytic activity. ([OPD] = 0.2 mM, [H₂O₂] = 10 mM, pH ~7.4, and temperature 37 °C were maintained during the experiments).

Table S5 Comparison of the OPD activity of B-CuNCs with other reported results.

Catalyst	Substrate	pH	Temperature (°C)	K_m (mM)	V_{max} (μMs^{-1})	References
MnO ₂ NPs	OPD	4	35	0.31	0.0821	S1
HRP	OPD	7	37	1.8	0.0012	S2
MnFe ₂ O ₄	OPD	7	25	27.5	0.104	S3
Cu-CDs	OPD	7	25	1.581	0.108	S4
Cu@Cu ₂ O aerogel	OPD	-	25	8.88	0.0237	S5
Phe-CuNCs	OPD	7.4	37	0.65	0.22	This Work



Scheme S1 The schematic representation of the peroxidase-like activity of B-CuNCs.

References:

- S1. X. Liu, Q. Wang, H. Zhao, L. Zhang, Y. Su and Y. Lv, *Analyst*, 2012, **137**, 4552-4558.
- S2. D. Yang, Q. Li, S. K. Tammina, Z. Gao and Y. Yang, *Sens. Actuators B*, 2020, **319**, 128273.
- S3. F. Vetr, Z. Moradi-Shoeili and S. Ö Zkar, *Appl. Organomet. Chem.*, 2018, **32**, 4465.
- S4. Q. Li, D. Yang, Q. Yin, W. Li and Y. Yang, *ACS Appl. Nano Mater.*, 2022, **5**, 1925-1934.
- S5. P. H. Ling, Q. Zhang, T. T. Cao and F. Gao, *Angew. Chem. Int. Ed*, 2018, **57**, 6819-6824.